32nd URSI GASS, Montreal, 19-26 August 2017

Frequency Tunable Graphene Metamaterial Reflectarray

S.H. Zainud-Deen[1], A.M. Mabrouk[2], and H.A. Malhat[1]
[1] Faculty of Electronic Engineering, Menoufia University, Menouf, 32952, Egypt
[2] Faculty of Engineering and Technology, Badr University in Cairo, Egypt

Abstract

In this paper, the radiation characteristics of frequency tunable graphene based metamaterial reflectarray have been investigated. The unit-cell consists of graphene two gaps split-ring-resonator (SRR) printed on a thick SiO_2 substrate. The metamaterial parameters of the unit-cell have been calculated at different graphene chemical potentials and different SRR gaps. Using waveguide simulator, the reflection coefficient phase of the graphene metamaterial reflectarray unit-cell has been investigated. A 13×13 graphene metamaterial reflectarray antenna fed by a circular horn antenna is designed and analyzed at different graphene chemical potentials. Full-wave analysis for the graphene metamaterial reflectarray antenna has been applied using the finite integration technique.

1. Introduction

Terahertz (THz) radiation provides many useful applications for spectroscopy, biomedical imaging, and security [1]. Metamaterials are artificial composite structures tailored electromagnetic response. Metamaterials are of particular interest in the terahertz regime, where the most nature materials exhibit only weak electric and magnetic responses and hence cannot be utilized for controlling the radiation. For practical applications, devices with large tunability are always preferred. Several methods have been examined in the literature to generate dynamic changes in the metamaterial's performance. These include direct changes in the unit cell's dimensions by varying capacitance or conductance, using electricity, chemically, thermally, or optically sensitive materials to change the constituent material properties of a structure and will change its electrical response and altering the geometry of the unit cell through stretching, shifting, or deforming all or parts of the structure. Some of these techniques, such as varactor diodes have been applied for operation at particular wavelengths, while others, such as phase-change materials have been applied across the electromagnetic spectrum [2]. Geometrical tuning can provide drastic changes in the metamaterial properties because the shape of the conducting elements has such a large influence on the corresponding resonance. While changing the shape of resonant elements provides a range of opportunities for tuning, the constituent materials that make up the unit cell ultimately control the properties of the metamaterial.

At terahertz frequencies, the plasmonic response becomes weak [3]. This restricts the use of noble metals in many THz applications [4]. Graphene, a thin layer of carbon atoms has been as an alternative candidate for plasmonics at THz band. Graphene is one million times thinner than paper and about 200 times stronger than steel. SiO_2 is the most common overlay material on silicon for enhancing the graphene layers. The electrical and mechanical properties of graphene, such as high mobility of electrons, low resistivity, high optical transparency, tunable conductivity and extreme mode confinement have made it a substantial substitution for noble metals in the field of plasmonic metamaterials [5].

A reflectarray comprises an array of reflective cells, introducing a given desired phase-shift upon reflection of the wave on the surface, offering the simplicity and highly efficient. Reflectarrays have a wide variety of applications in radar systems, radio astronomy observations and satellite communications. Tunable electromagnetic materials can be used as part of the construction of the reflectarray elements, enabling reflectarray become powerful beam-forming plate forms that combine the best features of aperture antennas and phased arrays [6].

In this paper, a tunable graphene metamaterial reflectarray, GMMRA, is proposed. Two gaps split-ring-resonator (SRR) element based on a graphene metamaterial at 0.81THz is designed as a unit-cell element in the reflectarray construction. Full-wave analysis using the finite integration technique is used to take into account the inter-element mutual coupling and assuming a local periodicity [7].

2. Numerical Results and Discussions

The structure of graphene metamaterial unit-cell element with its dimensions is shown in Fig.1.

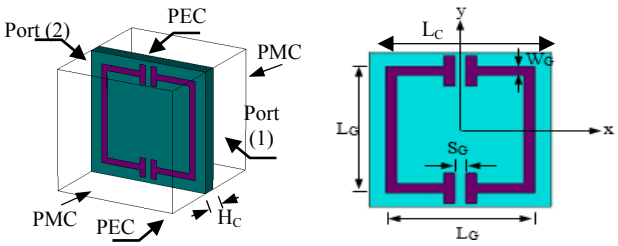

Figure 1. The structure of the graphene metamaterial unit cell with square SiO_2 substrate of L_C= 300 µm, L_G= 244.8 µm, W_G= 18 µm, S_G=14.4 µm and H_C= 30 µm.

The two gaps split-ring-resonator (SRR) is made from graphene-dielectric composites. The substrate is 30 μm thick SiO_2 with permittivity ϵ_r=3.9 [8]. It is found that the electrical conductivity of graphene can be controlled by changing the applied DC voltage. Graphene can be modeled as the infinitely thin surface of complex conductivity σ. It is represented by [9]:

$$\sigma(\omega) = \sigma_{intra}(\omega) + \sigma_{inter}(\omega) \quad (1)$$

where

$$\sigma_{intra}(\omega) \approx -j\frac{q_e^2 k_B T}{\pi\hbar(\omega - j2\Gamma)} \times \left(\frac{\mu_c}{k_B T} + 2\ln\left(e^{-\mu_c/k_B T} + 1\right)\right) \quad (2)$$

$$\sigma_{inter}(\omega) \approx -j\frac{q_e^2}{4\pi\hbar}\ln\left(\frac{2|\mu_c| - (\omega - j\tau^{-1})\hbar}{2|\mu_c| + (\omega - j\tau^{-1})\hbar}\right) \quad (3)$$

$\sigma_{intra}(\omega)$ is intraband term, $\sigma_{inter}(\omega)$ is the interband term, j is the imaginary unit, q_e is the electron charge, $\hbar = h/2\pi$ is the reduced Planck's constant, K_B is the Boltzman's constant, τ is the transport relaxation time, T is the temperature, ω is the operating angular frequency, the scattering rate $\Gamma = 1/2\tau$ represents loss mechanism, and μ_c is the chemical potential. The impedance of graphene can be efficiency controlled via a perpendicular bias electric field. The relationship between the applied electric field and the chemical potential, μ_c, can be calculated by [10].

$$E = \frac{q_e}{\pi\hbar^2 v_F^2 \varepsilon_o}\int_0^\infty \epsilon\left(f_d(\epsilon) - f_d(\epsilon + 2\mu_c)\right) d\epsilon \quad (4)$$

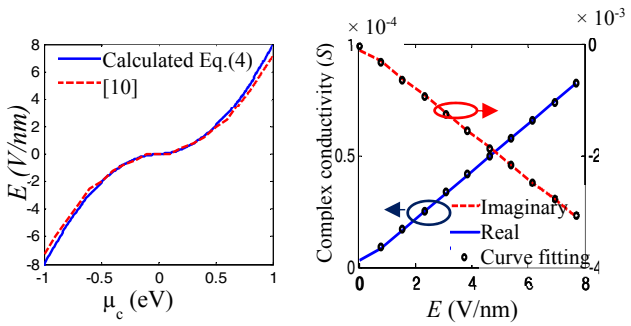

a. **b.**

Figure 2.a. The biasing electric field versus the chemical potential μ_c. **b**. Real and imaginary conductivity versus the bias electric field.

Figure 2a. shows the relation between the biasing electric field and the chemical potential calculated from Eq. (4) compared with that in Ref. [10]. The relationship between the complex conductivity and biasing electric field of the graphene sheet is shown in Fig. 2b. A curve fitting for the real and imaginary conductivity as a function of applied electric field is concluded as straight line from Eq. (5) and Eq. (6) and is given by [11]

$$\sigma_{Real} = p_1 E + p_2 \quad (5)$$

$$\sigma_{Img} = p_3 E + p_4 \quad (6)$$

where $p_1 = 1.0526\times10^{-5}$, $p_2 = 9.6588\times10^{-7}$, $p_3 = -3.97\times10^{-4}$, and $p_4 = -3.6413\times10^{-5}$.

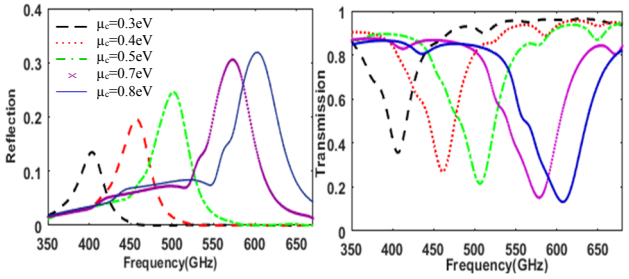

a. **b.**

Figure 3. a. The variation of the reflection $|S_{11}|^2$ and **b**. The transmission $|S_{21}|^2$ versus frequency of the graphene metamaterial unit cell.

The variations of the reflection, $|S_{11}|^2$, and the transmission, $|S_{21}|^2$, versus frequency of the graphene metamaterial unit cell are presented in Fig. 3 at different values of μ_c. The magnitude of the reflection and its resonance frequency are increased as the values of μ_c are increased. The S-parameters are related to both refractive index n and the impedance z as [12]

$$z = \pm\sqrt{\frac{(1+S_{11})^2 - S_{21}^2}{(1-S_{11})^2 - S_{21}^2}} \quad (7)$$

$$n = \frac{1}{kd}\cos^{-1}\left[\frac{1}{2S_{21}}(1 - S_{11}^2 + S_{21}^2)\right] \quad (8)$$

where n, k, and d denote the refractive index, the wave number of incident wave, and the thickness of the metamaterial slab, respectively. The permittivity (ϵ_r) and permeability (μ_r) are then directly calculated from ϵ_r=n/z and μ_r = n×z as shown in Fig. 4. The resonating reflection maximum shift from 400 GHz to 620 GHz covering a significant portion of the band. Figure 5 shows the variations of the same parameters at μ_c=0.5 eV for different values of the gap width S_G.

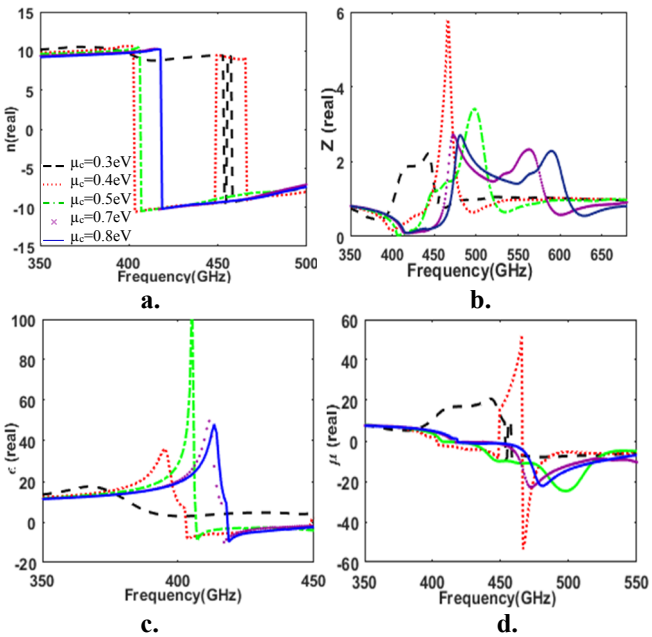

a. **b.**

c. **d.**

Figure 4. a. The variation of the refractive index, **b.** The impedance, **c.** The permittivity, and **d.** The permeability versus frequency of the graphene metamaterial unit cell at different values of μ_c.

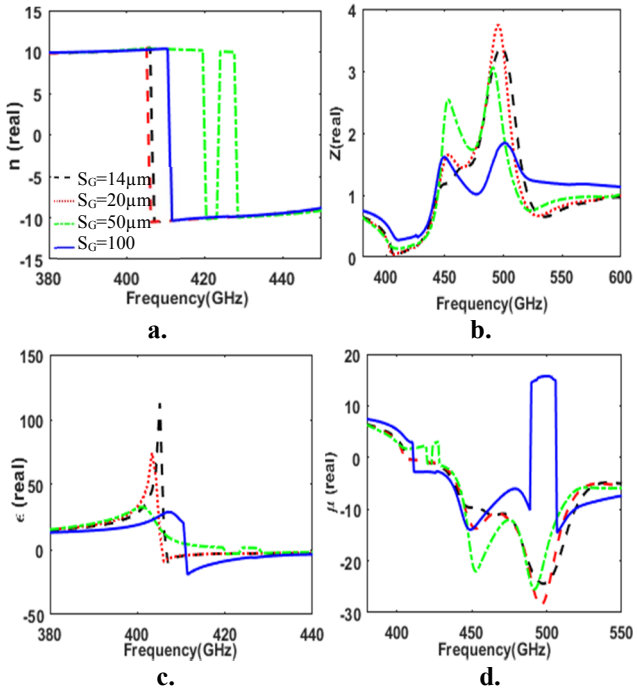

Figure 5. a. The variation of the refractive index, **b.** The impedance, **c.** The permittivity and **d.** The permeability versus frequency of the graphene metamaterial unit cell at different values of gap width S_G at μc=0.5 eV.

To design the graphene metamaterial reflectarray, the unit-cell element was placed in a waveguide simulator with perfect electric and magnetic wall boundary conditions to emulate an infinite periodic structure. A normal plane wave incident on a periodic infinite array of the reflectarray was assumed to determine the reflection coefficient of the unit cell. Figure 6 shows the reflection coefficient phase versus the gap width S_G at different values of μ_c. The phase range of beyond 316° is obtained when the gap width varies from 1 μm to 150 μm.

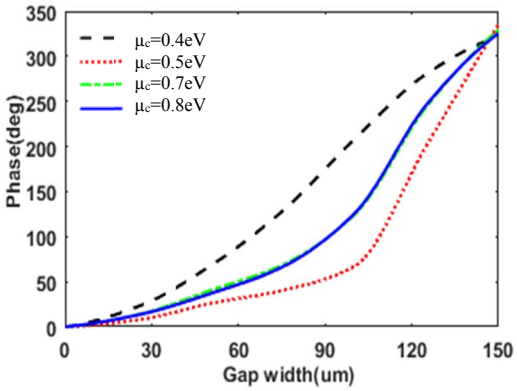

Figure 6. The variations of reflection coefficient phase versus the gap width of graphene metamaterial unit-cell element at different values of μ_c.

Figure 7 shows the geometry of a 13×13 GMMRA placed in x-y plane with total area 3.9×3.9 mm^2. A circular horn antenna located at a distance 3.9 mm (F/D=1) normal to the array aperture is used to feed the array structure. The phase-shift required at each unit-cell element in the reflectarray is calculated from [13],

$$\varphi_{ij}(x_{ij}, y_{ij}) = k_o(d_{ij} - \sin\theta_o(x_{ij}\cos\varphi_o + y_{ij}\sin\varphi_o)) \quad (9)$$

$$d_{ij} = \sqrt{(x_{ij} - x_f)^2 + (y_{ij} - y_f)^2 + (z_f)^2} \quad (10)$$

where φ_{ij} is the required reflected phase of the unit-cell at the position (x_{ij}, y_{ij}) to focus the reflected beam at deflection angles (θ_o, φ_o) and the is feed located at (x_f, y_f, z_f).

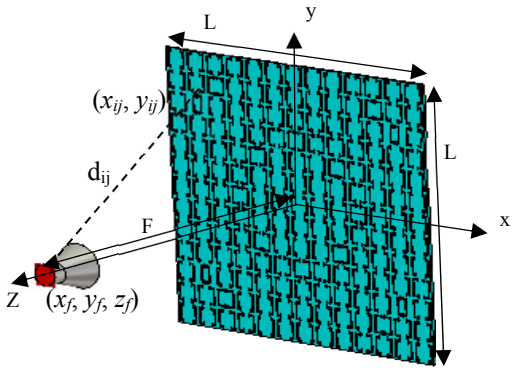

Figure 7. The structure of 13×13 graphene unit-cell reflectarray with L=F= 3.9 mm.

Figure 8 shows the 3-D radiation patterns for the reflectarray at different values of μ_c and operating frequencies. The gain variations versus frequency for the different reflectarrays are shown in Fig. 9. The maximum gain is 22.6 dB, 19 dB and 21.5 dB when μ_c equals 0.4 eV, 0.5 eV and 0.8 eV, respectively. The E and H-plane for different reflectarrays, at different values of μ_c, and operating frequencies are shown in Fig. 10. Approximately the same radiation patterns in different planes can be obtained by tuning the chemical potential μ_c.

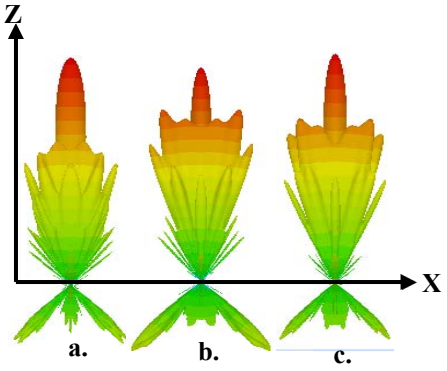

Figure 8. 3-D Radiation patterns:
a. μ_c =0.4eV, and f = 0.83 THz, **b.** μ_c =0.5eV, and f = 0.84 THz, and **c.** μ_c =0.8eV, and f = 0.85 THz.

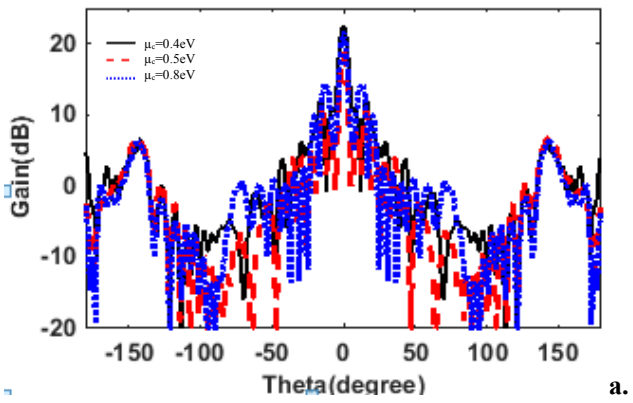

a.

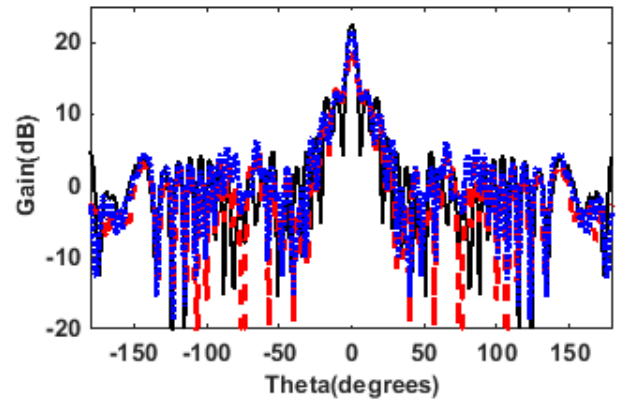

b.

Figure 10. Radiation patterns **a.** E-plane and **b.** H-plane.

3. Conclusions

This paper introduces a design of 13×13 GMMRA fed by circular horn for terahertz applications. The magnitude of the reflection and its resonance frequency are increased as the values of graphene chemical potential, μ_c, are increased. The unit-cell metamaterial properties, negative ε_r and μ_r are achieved in the frequency band from 400 GHz to 620 GHz for different μ_c and SRR gap width. The graphene metamaterial unit-cell element introduces a reflection coefficient phase variation of 316° for gap variation from 1 μm to 150 μm. A maximum gain of 22.6 dB was achieved at μ_c =0.4 eV. Approximately, the same radiation patterns in different planes are obtained by tuning the chemical potential μ_c.

4. References

1. J. Federici, and L. Moeller "Review of terahertz and subterahertz wireless communications," *Journal of Applied Physics,* vol. 11, pp. 107, July 2010. *doi: 10.1063/1.3386413*
2. N.T. Kadam, K.S. Janwalkar, A.A. Odhekar, "Parameter extraction for negative index metamaterials," *International Conference on Computer Technology, 2015.*
3. H. Tao, W.J. Padilla, X. Zhang, R.D. Averitt, "Recent progress in electromagnetic metamaterial devices for terahertz applications," *IEEE Journal on selected Topics in quantum Electronics*, vol. 17, pp. 92-101, 2011, *doi: 10.1109/JSTQE.2010.2047847.*
4. A. Andryieuski, and A.V. Lavrinenko, "Graphene metamaterials based tunable terahertz absorber: effective surface conductivity approach," *Optics Express,* vol. 21, pp. 9144-9155, 2013, *doi.org/ 10.1364/ OE.21.009144*
5. W. Bao, Electrical and mechanical properties of graphene, *Ph.D. Thesis, University of California, USA*, March 2012.
6. S.H. Zainud-Deen, H.A. Malhat, S.M. Gaber, M. Ibrahim, K.H. Awadalla, "Plasma reflectarray," *Plasmonics*, vol. 8, pp. 1469-1475, Dec. 2012. *doi: 10.1007/s11468-013-9560-8*
7. J. Shaker, M.R. Chaharmir, J. Ethier, Reflectarray Antennas, *Artech House,* 2013.
8. Liu and H.T. Hattori, " Tunable terahertz metamaterials based on ultra-subwavelength graphene-dielectric structures," *20th Microoptics Conference (MOC), Fukuoka*, pp. 1-2, 2015, *doi:10.1109/MOC.2015. 7416390.*
9. N. Rouhi, S. Capdevila, D. Jain, K. Zand, Y. Wang, E. Brown, L. Jofre, and P. Burke, "Terahertz graphene optics," *Nano Research Journal*, vol. 5, no. 10, pp. 667-678, Oct. 2012, *doi:10.1007/s12274-012-0251-0.*
10. G.W. Hanson, "Dyadic green's functions for an anisotropic, non-local model of biased graphene," *IEEE Trans. Antenna Propag.,* vol. 56, no. 3, pp. 747-757, 2008, *doi: 10.1109/TAP.2008.917005.*
11. W. M. Hassan, Analysis and design of high gain lens antennas, *Ph.D. Thesis, Faculty of Electronic Engineering, Menoufia University, Egypt*, 2016.
12. X. Chen, T. M. Grzegorczyk, B. I. Wu, J. Pacheco, and J. A. Kong, "Robust method to retrieve the constitutive effective parameters of metamaterials," *Physical Review E*, 70, 2004, pp. 016608-1:016608-7. *doi: 10.1103*/PhysRevE.70.016608.
13. Hend A. Malhat, S.H. Zainud-Deen, and S.M. Gaber, "Graphene Based Transmitarray for Terahertz Applications," *Progress In Electromagnetics Research M,* vol. 36, pp.185-191, January 2014. *doi: 10.2528/PIERM14050705*